Inhibitors of Protein−RNA Complexation That Target the RNA: Specific Recognition of Human Immunodeficiency Virus Type 1 TAR RNA by Small Organic Molecules

Houng-Yau Mei,*,‡ Mei Cui,‡ Andrea Heldsinger,§ Shannon M. Lemrow,‡ Joseph A. Loo,‡ Kristin A. Sannes-Lowery,‡ Lamia Sharmeen,§ and Anthony W. Czarnik‡,||

Department of Chemistry and Department of Therapeutics, Parke-Davis Pharmaceutical Research, Division of Warner-Lambert Company, 2800 Plymouth Road, Ann Arbor, Michigan 48106

Received June 17, 1998; Revised Manuscript Received August 12, 1998

ABSTRACT: TAR RNA represents an attractive target for the intervention of human immunodeficiency virus type 1 (HIV-1) replication by small molecules. We now describe three small molecule inhibitors of the HIV-1 Tat−TAR interaction that target the RNA, not the protein. The chemical structures and RNA binding characteristics of these inhibitors are unique for each molecule. Results from various biochemical and spectroscopic methods reveal that each of the three Tat−TAR inhibitors recognizes a different structural feature at the bulge, lower stem, or loop region of TAR. Furthermore, one of these Tat−TAR inhibitors has been demonstrated, in cellular environments, to inhibit (a) a TAR-dependent, Tat-activated transcription and (b) the replication of HIV-1 in a latently infectious model.

Drug discovery has traditionally involved a search for inhibitors of protein complexation to small molecules (e.g., substrates or ligands) or macromolecules (e.g., other proteins, nucleic acids, or polysaccharides). While agonists or antagonists of macromolecular receptors that become useful drugs must display a wide range of other attributes, including the appropriate physicochemical properties, pharmacokinetic and pharmacodynamic properties, stability, etc., they must first be protein ligands. The vast majority of available drugs act by binding noncovalently to a protein, preventing or (less often) stimulating that protein's complexation to a complement (*1*).

Complexes of nucleic acid and proteins are key intermediates in all transcriptional and translational processes. Some nucleic acids (e.g., ribozymes) even form functional complexes with small molecules (*2*). Nonetheless, nucleic acids are widely viewed as ineffective targets for the discovery of low-molecular weight inhibitors. One reason is that the linear motif in single-stranded DNA and the repetitive motif in double-stranded DNA provide attractive targets for large, linear binding molecules (*3*), but unattractive targets for the small molecules that lead to orally available medications. Another reason is that the lack of tertiary structure in DNA does not afford the diverse topology associated with folded proteins.

However, single-stranded RNA often folds into well-defined tertiary structures (*4*). Furthermore, such structures serve as docking sites for transcriptional activators (*5*) and substrates for self-splicing reactions (*6*, *7*). Can such structured nucleic acids display sufficient shape diversity to permit the complexation of a small molecule at one site in a virtual sea of nucleic acid material? This is the essential question whose presumed negative answer hinders drug discovery at the nucleic acid level.

Certain cis-acting RNA elements are essential for the gene expression of human immunodeficiency virus type 1 (HIV-1) (*8*). The functions and sequences of these RNA molecules have been well characterized (*9*−*11*). A segment of HIV-1 mRNA (residues 1−59), identified as the transactivation responsive element (TAR), adopts a stem−loop secondary structure consisting of a highly conserved hexanucleotide loop and a three-nucleotide bulge flanked by two double-stranded stems (*12*, *13*). HIV-1 encodes a regulatory protein, Tat, for interacting with TAR and activating both the initiation and elongation processes of transcription (*14*−*16*). While U_{23} of the bulge serves as the marker for Tat recognition, the hairpin loop provides a homing site for other cellular proteins (*12*). Both are important for the formation of processive transcription complexes through specific protein−RNA interactions (*14*−*16*). Deletion of either bulge or loop residues of TAR impairs the transcription and, subsequently, the replication of HIV-1 (*5*, *12*). HIV-1 TAR RNA and its cellular functions, therefore, represent a potential target for therapeutic intervention (*17*−*19*).

In this paper, we report that multiple small molecule inhibitors can be identified for the HIV-1 Tat−TAR system, each sufficiently potent to evoke interest in initiating a structure−activity relationship (SAR) study. Furthermore, these three small molecule inhibitors bind to TAR at three distinct sites, as characterized by footprinting methods. Each of these inhibitors has been shown to recognize the TAR structure preferentially over other nucleic acids.

* To whom correspondence should be addressed. E-mail: Houng-Yau.Mei@wl.com.

‡ Department of Chemistry.

§ Department of Therapeutics.

|| Present address: Illumina, 9390 Towne Centre Drive, San Diego, CA 92121.

S0006-2960(98)01308-7 CCC: $15.00
Published on Web 09/17/1998

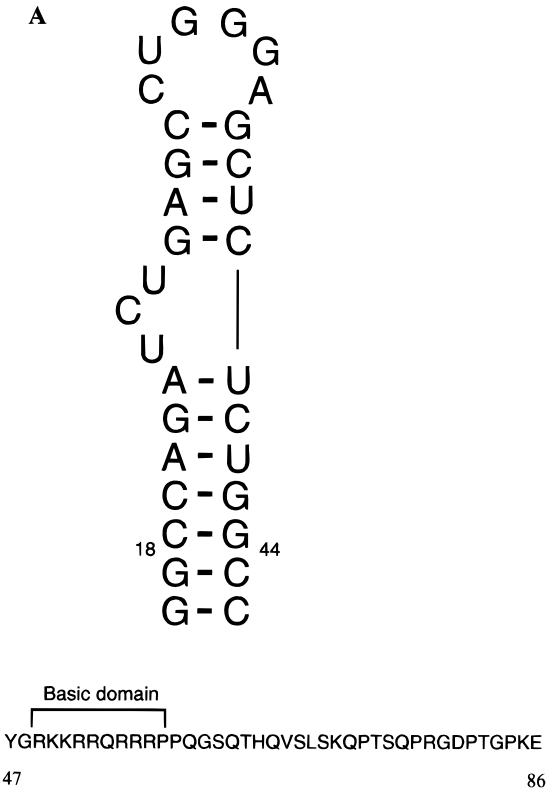

FIGURE 1: (A) Sequence and secondary structure of TAR RNA. TAR_{31}, containing residues 18−44 of HIV-1 mRNA and two additional G•C base pairs, was used in this study. (B) Sequence of the Tat-derived peptide. The Tat_{40} peptide contains amino acid residues 47−86 of the HIV-1 Tat protein.

EXPERIMENTAL PROCEDURES

Materials. Tat_{40} and TAR_{31} (Figure 1) were chemically synthesized and purified as described previously (*19*). RNA was labeled either at the 3′-end with [5′-^{32}P]pCp using T4 RNA ligase or at the 5′-end with [γ-^{32}P]ATP using T4 polynucleotide kinase. All RNA samples were renatured by heating to 90 °C for 5 min followed by slow cooling to room temperature. The proper folding of a ^{32}P-labeled TAR RNA was determined on the basis of its binding affinity for Tat_{40} or neomycin. Similar binding affinities (0.5 nM for Tat_{40} or 1 μM for neomycin) determined by the mobility shift method (*19*) were found for both 3′- and 5′-end-labeled TAR.

Electrospray Mass Spectrometry. ESI-mass spectrometry was performed with a double focusing hybrid mass spectrometer (EBqQ geometry, Finnigan MAT 900Q, Bremen, Germany). A stream of SF_6 coaxial to the spray suppressed corona discharges, especially important for ESI of aqueous solutions. Solution flow rates for delivery to the ESI source were in the 0.15−1.0 μL min^{-1} range. RNA solutions were buffered with 10 mM ammonium acetate (pH 6.9) and were annealed by heating for 4 min at 95 °C and cooled slowly (3−4 h). Methanol (10% v/v) and 1,2-diaminocyclohexane-*N*,*N*,*N*′,*N*′-tetraacetic acid (CDTA) were also added to the aqueous ammonium acetate ESI-MS solutions. The addition of methanol enhanced the stability of the ESI-MS signal. The extent of adduction of cations from ubiquitous salts by RNA was reduced by ethanol precipitation of RNA and by the addition of CDTA.

Ribonuclease Footprinting Experiments. In a typical experiment, 20 μL of a 5% DMSO/H_2O buffer containing 25 mM Tris-HCl (pH 7.5), 10 mM $MgCl_2$, 200 mM NaCl, 1 μg of yeast tRNA (Sigma), and ^{32}P-labeled TAR_{31} (∼30000 cpm) was incubated with either 2×10^{-3} units of RNase V1 (Amersham) or RNase A (3.6 pg/μL, Sigma) at room temperature for 10 min in the presence of the inhibitor at various concentrations. After incubation, to samples was added 10 μL of formamide loading dye and the samples were electrophoresed on a 20% polyacrylamide denaturing (7 M urea) gel for 3 h.

Chemical Probe Footprinting Experiments. The procedure for DEPC modification experiments is as follows. To a 35 μL 5% DMSO/H_2O solution of 80 mM HEPES (pH 7.3), 100 mM KCl, 0.1 mM EDTA, 1 μg of yeast tRNA, and 3′-^{32}P-labeled TAR_{31} (∼80000 cpm) was added 5 μL of DEPC (Sigma) and the mixture incubated at room temperature for 10 min in the presence of **2** at various concentrations. The reaction was stopped by adding 4 μL of 3 M NaOAc (pH 5.3) and 160 μL of ethanol and the mixture precipitated at −20 °C for 30 min. After ethanol precipitation, dry pellets were redissolved in 20 μL of aniline/acetic acid (1:1 v/v) and the mixture was incubated at 55 °C for 30 min, followed by two repeats of ethanol precipitation with 300 μL of 0.3 M NaOAc and 1 mL of ethanol or 300 μL of 70% ethanol. RNA pellets were dissolved in formamide loading dye and electrophoresed on a 20% polyacrylamide denaturing gel for 3−4 h. The procedure for DMS modification experiments is as follows. To a 39 μL 5% DMSO solution of 80 mM HEPES (pH 7.3), 100 mM KCl, 0.1 mM EDTA, 1 μg of yeast tRNA, and 3′-^{32}P-labeled TAR_{31} (∼100000 cpm) was added 1 μL of DMS (Sigma) and the mixture incubated at room temperature for 10 min. The reaction was stopped by adding 4 μL of 3 M NaOAc (pH 5.3) and 160 μL of ethanol and the mixture precipitated at −20 °C for 30 min. After ethanol precipitation, dry pellets were redissolved in 10 μL of 0.2 M $NaBH_4$ (7.6 mg/mL, freshly prepared) and incubated in an ice bath for 30 min. After incubation, the reaction was stopped by ethanol precipitation. Dry RNA pellets were redissolved with 20 μL of aniline/acetic acid (1:1 v/v), and the mixture was incubated at 55 °C for 30 min, followed by two repeats of ethanol precipitation with 300 μL of 0.3 M NaOAc and 1 mL of ethanol or 300 μL of 70% ethanol. RNA pellets were dissolved in formamide loading dye and electrophoresed on a 20% polyacrylamide denaturing gel for 3−4 h.

Anti-Tat Transactivation Assays. The HIV-1 Tat gene was introduced into HeLa cells by stable transfection of plasmid RSV-Tat-Neo (a gift from M. Peterlin, University of California, San Francisco, CA). This was followed by clonal selection with G418. Cells expressing HIV-1 Tat were confirmed by Western blot analysis with a rabbit polyclonal anti-Tat antibody (ABT). For these HeLa-tat cells, pLTR-*lacZ* plasmids in which the expression of *lacZ* is under the control of HIV-1 3′ LTR (AIDS Reference Reagent Program) and pCMV-*lacZ* plasmids in which *lacZ* expression is under the control of the CMV promoter (a gift from M. Levine, University of Michigan, Ann Arbor, MI) were used for further transfections. Transient transfection of plasmid pLTR-*lacZ* or CMV-*lacZ* was carried out by electroporation. An aliquot of 5 μg of plasmids was added to 4×10^6 HeLa-tat cells, and the cells were electroporated at 230 V and 960 μF using a Gene Pulser (Bio-Rad). Cells were then plated in a 96-well plate with 10^4 cells in each well. Inhibitors

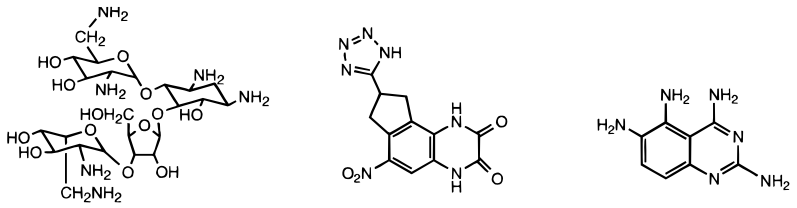

Tat/TAR Inhibitors	**1**	**2**	**3**
IC_{50} values	0.92 ± 0.09 μM	1.3 ± 0.1 μM	10 ± 1 μM

FIGURE 2: Chemical structures and IC_{50} values of three small molecule Tat−TAR inhibitors. IC_{50} values were obtained using gel mobility shift assays as described previously (*19*). All inhibition studies were performed in a buffer solution containing 10 mM Tris-HCl (pH 7.5), 70 mM NaCl, 0.2 mM EDTA, 0.01% Nonidet P-40, 5% glycerol, and ~100 pM 3′-end ^{32}P-labeled TAR. The IC_{50} value for **1** was determined in the presence of 0.5 nM Tat, while IC_{50} values for **2** and **3** were obtained in the presence of 1 nM Tat. Each IC_{50} value is a mean (with standard error) from at least three independent experiments.

were added to the medium at appropriate concentrations. Cells were incubated at 37 °C for 48 h, after which reactions were stopped by addition of 100 μL of reporter lysis buffer (Promega) to each well. The extent of expression of β-galactosidase was determined by a colorimetric assay following the addition of 100 μL of assay buffer [80 mM sodium phosphate buffer (pH 7.4), 102 mM 2-mercaptoethanol, 9 mM $MgCl_2$, and 8 mM chlorophenol red-β-D-galactopyranoside, Promega] to each well. Plates were incubated at 37 °C for 30 min, and the absorbance in each well was measured at 570 nM. The effect of the compound on cell viability was examined by a standard tetrazolium test with the addition of 0.3 mM XTT [2,3-bis(2-methoxy-4-nitro-5-sulfophenyl)-2*H*-tetrazolium-5-carboxanilide inner salt, Sigma].

Anti-HIV-1 Replication Assays. OM-10.1 cells were obtained from the AIDS Reference Reagent Program. OM-10.1 cells were activated with 2 units/mL TNF-α and seeded in 96-well plates. Serial dilutions of compounds were added to the wells at the same time. Cells were grown at 37 °C for 48 h in the absence or presence of drugs. The extent of viral expression in the cell line was determined by the measurement of the extent of p24 production (p24 ELISA assay kit, Coulter Immunology) in the cell-free supernatant medium.

RESULTS AND DISCUSSION

Identification of Three Small Molecule Tat−TAR Inhibitors That Bind to RNA. We have previously reported a drug discovery approach (*19*) designed to identify small organic molecules that inhibit HIV-1 replication by blocking Tat−TAR interaction. As shown in Figure 1, the sequences of TAR_{31} (containing residues 18−44 of HIV-1 mRNA) and Tat_{40} peptide (residues 47−86), each containing the key element for protein−RNA recognition, were used in these studies. The first step of this approach utilizes methodologies such as gel mobility shift, membrane filtration, and scintillation proximity assays to search for inhibitors of HIV-1 Tat−TAR binding. Such methods constitute common ways of screening for small molecules that bind to proteins. Small organic compounds from our research compound library were utilized as the source of molecular diversity.

From this drug screening program, we have identified several series of small molecules that block Tat from binding to TAR. Aminoglycoside antibiotics, quinoxaline-2,3-diones, and 2,4-diaminoquinozalines have been found to be potent inhibitors. Among them, aminoglycoside antibiotics have previously been reported (*20*) to exert their antibacterial functions by interacting with the decoding region of ribosomal RNA. There has been significant interest in understanding the details of how these antibiotics interact with various RNA targets (*21*). Only few prior reports (*22*−*26*), however, have been found that identify small molecules as inhibitors of any protein−RNA interactions.

Examples of the three Tat−TAR inhibitor series and their IC_{50} values are presented in Figure 2. Neomycin (**1**), 2,3-dioxo-8-[2-(5-tetrazolyl)]-2,3,4,7,8,9-hexahydro-1*H*-6-nitrocyclopenta[*f*]quinoxaline (**2**), and 2,4,5,6-tetraaminoquinozaline (**3**) represent three different small molecule inhibitors of the Tat−TAR interaction with IC_{50} values of 0.92 μM. Further studies have now shown a wide range of Tat−TAR inhibitory activities (IC_{50} values of sub-micromolar to millimolar) exist among analogues within each series.

Inspection of the structures of these three Tat−TAR inhibitors shows no apparent similarity. Therefore, it is likely that the molecular target (protein or RNA) and/or the specific interaction sites for these three molecules may be different. Although our drug screening approach has the potential to select anti-HIV agents that function at the Tat−TAR interaction, the assays we employed did not distinguish among inhibitors interacting with Tat, TAR, or both. To address this question, electrospray ionization mass spectrometry (ESI-MS) was used. ESI-MS has been previously reported to detect noncovalent interactions between small molecules and macromolecules such as proteins or nucleic acids (*27*, *28*). The formation and stoichiometry of the small molecule−macromolecule complexes can be deduced by mass measurement. We have previously demonstrated that ESI-MS experiments examining the Tat−TAR or aminoglycoside−TAR interaction are consistent with solution studies (*29*, *30*).

As shown in Figure 3, molecular weights corresponding to TAR alone and TAR and its 1:1 stoichiometry complexes with **1**, **2**, or **3** were measured by ESI-MS. At higher drug concentrations, nonstoichiometric complexes were also evident for all three inhibitors. Under similar conditions, no complexes with a Tat_{40} peptide were found for any of these small molecules. Furthermore, from ESI-MS measurements, addition of these small molecules to preformed the Tat−

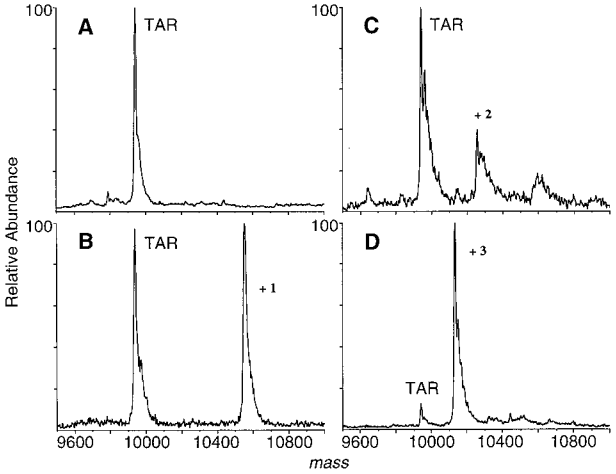

FIGURE 3: Deconvoluted negative ion electrospray ionization mass spectra of (A) TAR RNA (M_r = 9941), (B) TAR RNA and **1** (1:1 molar ratio), (C) TAR RNA and **2** (1:15 molar ratio), and (D) TAR and **3** (1:1.5 molar ratio).

TAR complex resulted in TAR−drug complexes and dissociation of the Tat−TAR complex. These results strongly suggest that, although different binding characteristics may exist, all three Tat−TAR inhibitors interact with TAR but not with Tat at the concentrations resulting in binding inhibition.

We have reached the following conclusions concerning the mechanisms of TAR binding by the small molecule inhibitors.

*(1) Inhibitor **1** Binds to the Lower Stem Region of TAR RNA and Inhibits Tat−TAR Interaction through an Allosteric Mechanism*. Once the RNA had been identified as the molecular target, we conducted out experiments to reveal the binding characteristics of these inhibitors. Previous competition studies (*29*−*31*) suggested that **1** can complex preferentially to TAR in comparison with other nucleic acids, including (a) tRNA, (b) double-stranded homopolymers of DNA or RNA, and (c) single-stranded RNA. Furthermore, mutations at the bulge or loop domains of TAR seem to have little or no effect on the extent of **1** binding (*31*).

To identify the primary binding site for **1**, we performed high-resolution mapping experiments using ribonucleases V1 and A. This experiment is difficult because only a few small molecule RNA ligands (e.g., aminoglycoside antibiotics) have previously been mapped using the footprinting techniques (*31*, *32*). Notwithstanding concerns such as the efficiency of nucleases, the disruption of RNA−ligand interaction, the association−dissociation behavior of the ligands, and the quantitation of protection, footprinting experiments reveal key elements involved in a RNA−ligand interaction. The V1 degradation pattern of a 3′-^{32}P end-labeled TAR is shown in Figure 4A. In the absence of any drug (lane 3), residues 41−43 in the lower stem region and in the bulge region (residue 24) were preferentially cleaved by V1. Hydrolysis by RNase V1 at the three-nucleotide bulge was previously reported (*31*). The cleavage at nucleotide 24 can be attributed to extended stacking of the bulge residues with neighboring helical stems. This result was also supported by recent NMR studies (*33*). Lanes 4−7 reveal that V1 degradation of these residues is inhibited in a dose−response manner by the addition of **1**. Protection of these residues indicates a "footprint" for **1** spanning from

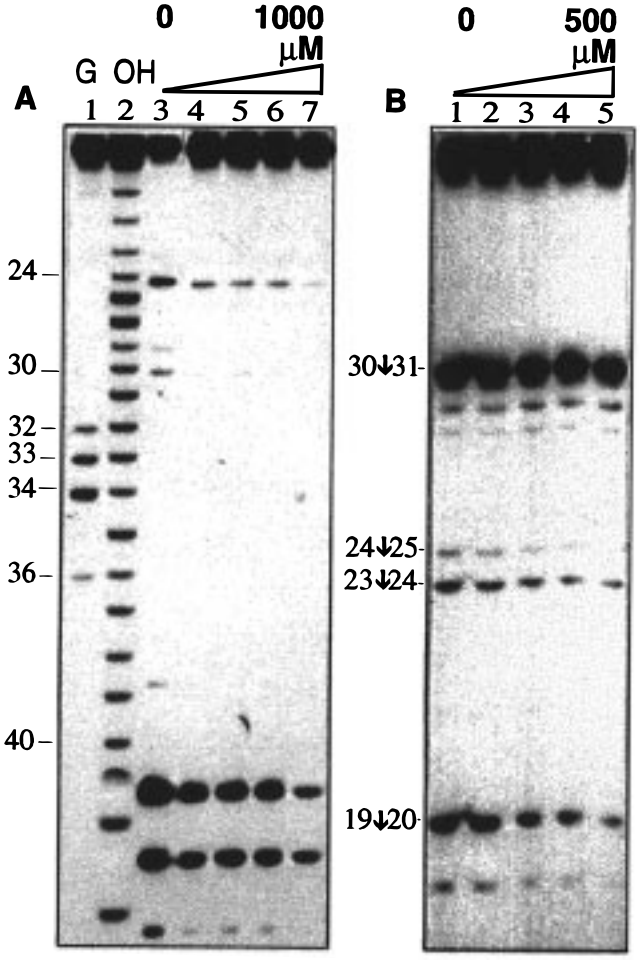

FIGURE 4: Protection of TAR RNA from nuclease degradation by **1**. (A) Nuclease V1 cleavage of 3′-^{32}P end-labeled TAR protected by **1** (neomycin sulfate, Sigma). Lane 1 represents the G-specific reactions (residue numbers indicated), and lane 2 represents the alkaline hydrolysis reaction of the TAR_{31}. Lanes 3−7 represent the RNase V1 degradation reaction in the presence of **1** at 0, 20, 100, 200, and 1000 μM, respectively. (B) RNase A cleavage of 5′-^{32}P end-labeled TAR protected by **1**. Lanes 1−5 represent the RNase A degradation reaction in the presence of **1** at 0, 10, 50, 100, and 500 μM, respectively. Phosphodiester bonds cleaved by RNase A are indicated.

the lower duplex region to part of the bulge of TAR. This observation was further supported by RNase A footprinting experiments on a 5′-^{32}P end-labeled TAR. In Figure 4B, the most significant protection by **1** was found at the C_{19} residue (located in the lower stem region.)

Footprints in these mapping experiments indicate that small molecules protect the RNA residues from nuclease degradation. The protections, as shown in Figure 4, can be attributed to either direct contacts between small molecules and RNA or an allosteric effect induced by the binding of small molecules. In the case of **1**, the allosteric mechanism was supported by (a) circular dichroism (CD) studies (*31*) that indicated a conformational change of TAR and dissociation kinetics and (b) ESI-MS experiments (*34*) that strongly suggested the formation of a ternary complex of **1**, Tat, and TAR. On the basis of these results, we proposed a noncompetitive inhibition mechanism for **1**. **1** binds primarily to the lower stem region of TAR that is not occupied by Tat, and the binding of **1** facilitates the departure of Tat from TAR. To the best of our knowledge, **1** represents the first

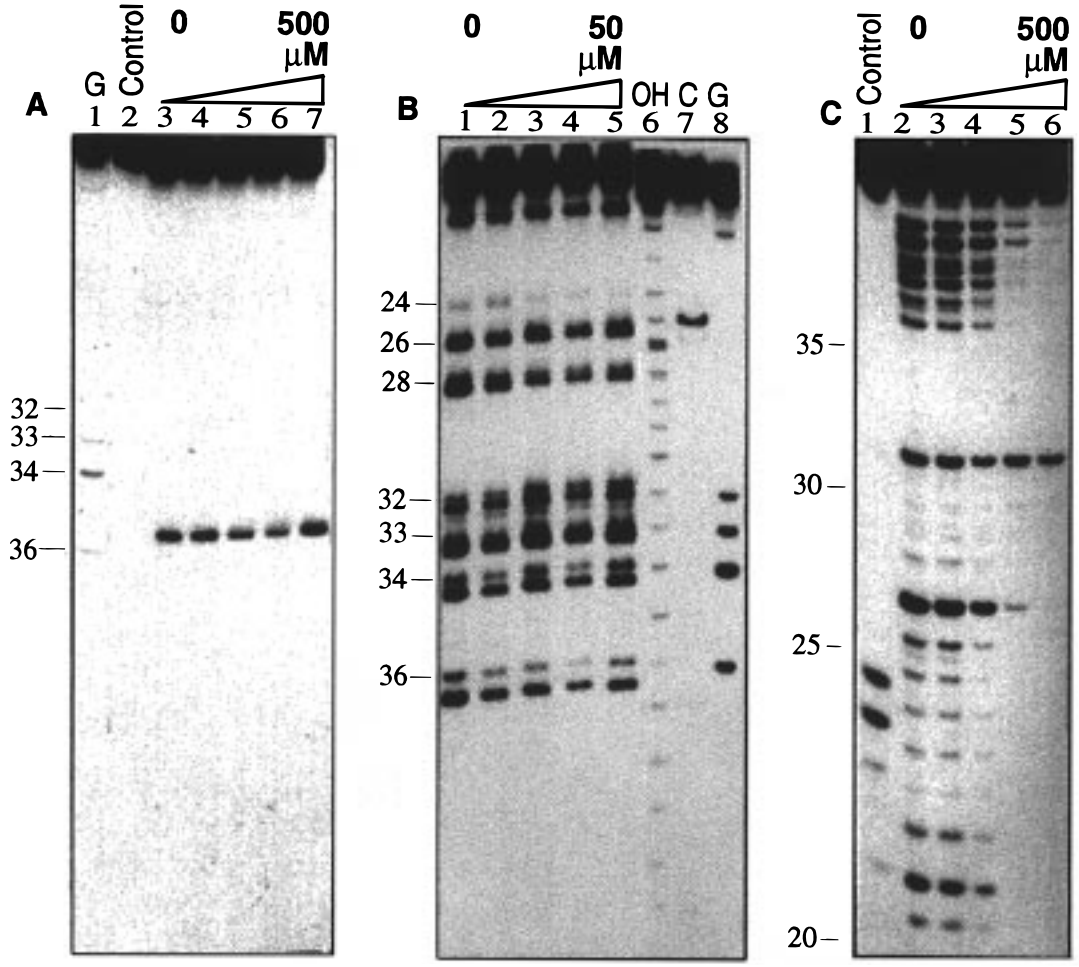

FIGURE 5: Protection of TAR RNA from nuclease degradation by **2**. (A) DEPC protection analysis. Lane 1 represents the G reaction, and lane 2 is the TAR control without any treatment. Lanes 3−7 represent DEPC modification of TAR in the presence of **2** at 0, 10, 50, 100, and 500 μM, respectively. (B) DMS protection analysis. Lanes 1−5 represent DMS modification of TAR in the presence of **2** at 0, 1, 5, 10, and 50 μM, respectively. Lane 6 shows alkaline hydrolysis of TAR, and lanes 7 and 8 represent C and G reactions, respectively. Aniline reaction at the DMS-modified residues generated truncated 3′-end-labeled RNA fragments, each with a phosphate group at the 5′-end. Partial hydrolysis of the 5′-phosphate group can be attributed to the doublet bands seen for each of these RNA fragments in the figure. (C) V1 nuclease protection analysis. Lane 1 shows a control sample of a 5′-^{32}P end-labeled TAR without any treatment. Lanes 2−5 show V1 cleavage of this RNA in the presence of **2** at 0, 1, 10, 100, and 500 μM, respectively. The residue assignment is based on alkaline hydrolysis and RNA sequencing reactions of TAR. The fact that more than four bands were observed between residues 20 and 25 may be due to the existence of some shorter fragments (evident in the figure) of the 5′-end-labeled RNA. This "doublet" cleavage pattern was clearly revealed only after V1 cleavage. Bands representing the same hydrolyzed product of the ^{32}P-labeled TAR can be easily distinguished from others because of their similar mobility and concurrent intensity changes upon V1 hydrolysis. This pattern was reproducible and did not affect our qualitative analysis. For quantitative analysis (results shown in Figure 6), the intensities of both doublet bands (shorter fragments usually have less than 20% of the total intensity) were added up to represent the extent of cleavage at the corresponding residue.

example of a noncompetitive small molecule inhibitor for the Tat−TAR interaction.

*(2) Inhibitor **2** Makes Specific Contacts with the Bulge Region of TAR and Competitively Inhibits Tat Binding to TAR*. We have also studied the binding characteristics of **2** using nuclease-protection methods. Both chemical nucleases such as diethyl pyrocarbonate (DEPC) and dimethyl sulfate (DMS) and ribonuclease V1 were used. DEPC specifically modifies residue A_{35} (Figure 5A) of TAR, while DMS is highly reactive toward guanines (residues 26, 28, 32−34, and 36) and moderately reactive toward residue C_{24} (Figure 5B). Figure 5A reveals that chemical modification of loop residue A_{35} is not affected by the addition of **2**. Similarly, no protection was found for guanine residues at either the loop or the double-helical regions (Figure 5B). However, as shown in lanes 2−5 of Figure 5B, DMS methylation at bulge residue C_{24} was greatly affected, in a dose−response manner, by the presence of **2**. At very high concentrations (for example, 500 μM) of **2**, secondary protection was observed for residues 26 and 28.

The binding sites occupied by **2** were further elucidated using V1 footprinting experiments. As shown in Figure 5C, most of the stem region (residues 19−22, 26−28, 36−39, and 40−42), bulge residues 23−25, and loop residue 31 are cleaved by V1 nuclease. By comparison, in the presence of increasing concentrations of **2** (lanes 2−5), a dose−response protection on all but U_{31} residues is evident. The fact that the V1 cleavage at U_{31} was not affected by the addition of **2** suggests that the loop region is not involved in the binding of **2**. In addition, densitometric quantitation of these results shows that the most significant protection (residues 25 and 26) centers around the bulge region of TAR. Both DMS and V1 footprinting results are therefore consistent with a binding model in which the bulge region of TAR is the major binding site for **2**.

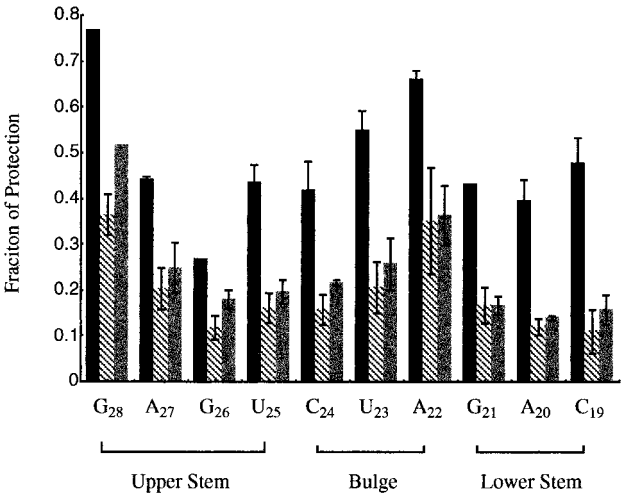

FIGURE 6: Selectivity studies of **2**. The percentage of V1 cleavage (*y*-axis, relative to the total amount of [^{32}P]TAR used) is shown for TAR residues 19−28 (*x*-axis). A higher percentage of V1 cleavage represents less protection by **2**. As described in Figure 5C, in the presence of 100 nM nonradioactive carriers, V1 cleavage of a 5′-^{32}P end-labeled TAR was performed. For each residue, the fraction of V1 cleavage in the presence of different carriers, TAR (black columns), tRNA (gray columns), or calf thymus DNA (hatched columns), is shown. The extent of V1 cleavage of each residue in the presence of one type of carrier was quantitated using a phosphoimager (Molecular Dynamics). To normalize the effect of V1 on different carriers, the fraction of V1 cleavage was determined by dividing the absolute extent of cleavage at each residue in the presence of drug (100 μM of **2**) by that of the control (RNA only) under the same conditions. The data are expressed as the mean and standard error of the mean from three separate experiments. The binding preference of **2** for TAR is clearly evident.

Since the primary footprint of **2** coincides with the known binding site of Tat, we have studied the effect of **2** on the dissociation kinetics of Tat. In contrast to **1**, **2** was found to inhibit the Tat−TAR interaction without affecting the dissociation off-rate of bound Tat. This and footprinting results together suggest a competitive mechanism for **2**. **2** inhibits Tat−TAR interaction by binding to the same site of the TAR bulge that Tat recognizes. We have also found that **2** inhibits Tat binding to HIV-2 TAR (with a UU bulge) with an IC_{50} value similar to that of HIV-1 TAR. This suggests that **2** recognizes a specific conformation of the bulge region, not the sequence of TAR bulge.

To become a useful drug candidate, any Tat−TAR inhibitor must show reasonable selectivity for TAR versus other nucleic acid molecules. To address this issue, V1 footprinting experiments of **2** were performed in the presence of various carrier nucleic acids, including TAR, yeast tRNA, and calf thymus DNA. In these studies, tRNA and calf thymus DNA serve as examples of nonspecific RNA and DNA, respectively. If nonradioactive carriers would compete for **2** with [^{32}P]TAR, the extent of footprinting by **2** would be reduced and the relative binding preference of **2** could therefore be deduced. This was the case. Figure 6 shows V1 cleavage of a ^{32}P-labeled TAR protected by **2** in the presence of different carrier nucleic acids. Under these conditions, the extent of protection by **2** was found to vary when different carriers were used. This evidence supports the possibility that the drug exerts its protection by binding to TAR (at least partially), but not by affecting the activity of the nuclease. More importantly, as evident in most residues, the amount of nuclease V1 protection on [^{32}P]TAR was reduced most significantly in the presence of cold TAR. These results strongly suggest that **2** has a binding preference for TAR, at least qualitatively, as compared to tRNA or calf thymus DNA.

*(3) Inhibitor **3** Inhibits the Tat−TAR Interaction by Binding to the Loop Region of TAR, Downregulates Cellular Tat Transactivation, and Ultimately Inhibits HIV-1 Replication*. As described previously, we have investigated the binding characteristics of **3** using nuclease-protection methods. Figure 7A shows the DEPC footprinting data of **3**. In contrast with the results of **2**, DEPC modification at loop residue A_{35} was strongly protected by **3**. The extent of protection was found to be dose-dependent, with a 30% protection level at 10 μM **3** and a greater than 80% protection level at 50 μM under our experimental conditions. The protection was also specific for A_{35}. No apparent protection was found at the two weakly modified residues, A_{22} and A_{27}.

Binding of **3** in the vicinity of A_{35} is further supported by the DMS footprinting data. As shown in Figure 7B, **3** protects residue G_{36} from DMS modification. At 100 μM, about 30% of the DMS methylation at G_{36} was protected by **3**. Under similar conditions, modifications at guanine residues 21, 26, 28, and 32−34, or at C_{24} in the bulge region, were not affected by the presence of **3**. At higher concentrations, e.g., [**3**] = 500 μM, some (∼30%) secondary protection was found for G_{26} and G_{28}, both located in the upper stem region. Interestingly, guanine residues in the loop region were not protected by **3** under any condition. Furthermore, unlike **2**, **3** does not protect any residues (including stem residues and C_{30} and U_{31} in the loop) from V1 degradation (Figure 7C). These results suggest that the 3′-end of the TAR loop and the neighboring base pairs are essential for **3** binding.

Footprinting results of **3** were further supported by ESI-MS studies. The competition of **3** for the wild type and linker-loop TAR has been studied by ESI-MS. Prior to studies with **3**, we have first determined that the binding affinities for Tat with wild type or linker-loop TAR [TAR_{31} with the hexanucleotide loop replaced by a polyethylene glycol linker ($O[(CH_2)_2O]_4(CH_2)_2O$)] are essentially the same. This indicates that both RNA molecules share a similar structure (UCU bulge flanked by two double-helical stems) that is recognized by Tat. Also, as shown in Figure 8A, almost quantitative signals corresponding to 1 equiv of each RNA can be measured by ESI-MS. However, when this 1:1 mixture of wild type and linker loop TAR was added to 2 equiv of **3**, only wild type TAR formed a complex with **3** (Figure 8B). These results indicate an important role for the loop in binding with **3**.

We have investigated the cellular activity of the Tat−TAR inhibitors using a Tat-activated reporter gene assay. This assay utilizes a HeLa cell line constitutively expressing HIV-1 Tat proteins and a reporter system in which the expression of the *lacZ* gene is driven by the HIV-1 LTR promoter (*19*). The cellular efficacies of Tat−TAR inhibitors were determined by measuring the amount of β-galactosidase in the presence of these inhibitors compared with controls. As shown in Figure 9A, **3** shows a dose−response inhibitory effect on the expression of *lacZ* with an EC_{50} value of 19 μM. There was no apparent cellular toxicity at drug concentrations below 100 μM. Furthermore, in a similar cellular environment, **3**'s inhibitory effect on TAR-indepen-

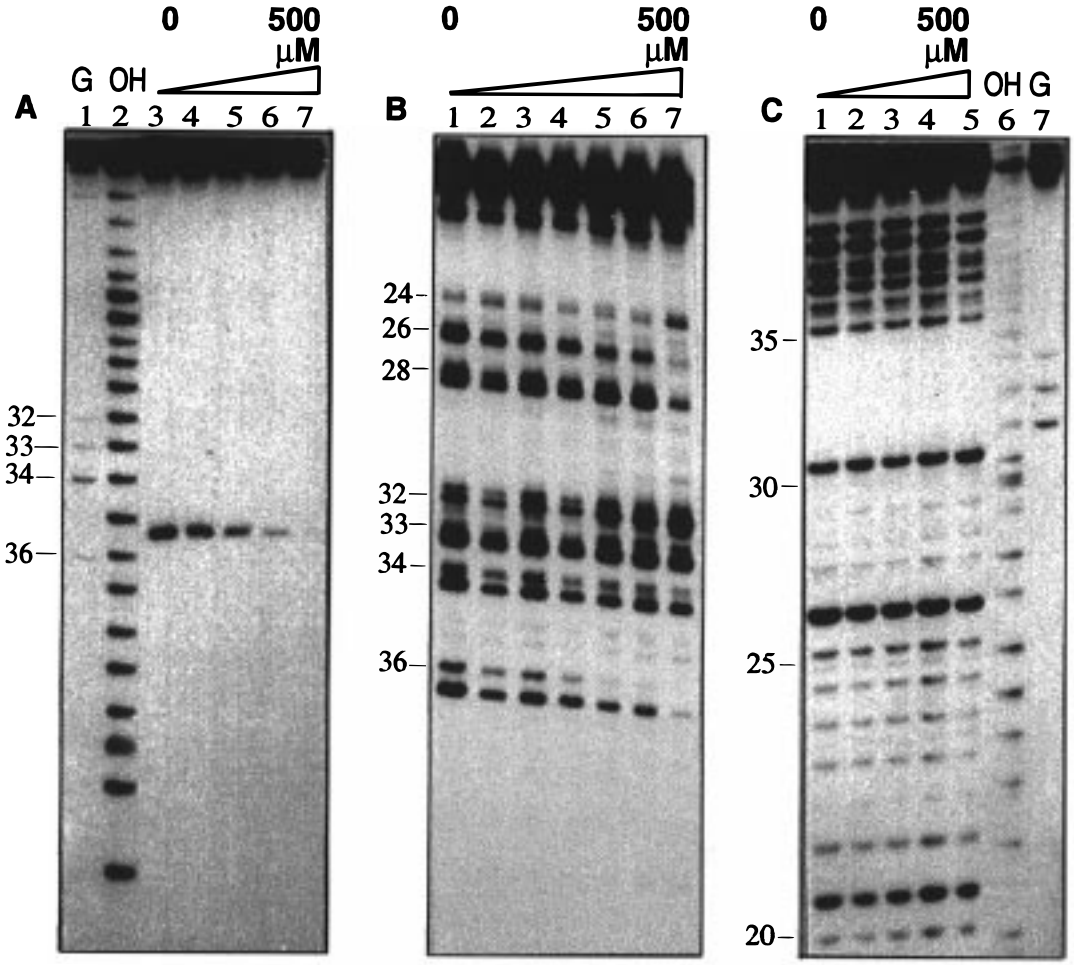

FIGURE 7: Protection of TAR RNA from nuclease degradation by **3**. (A) DEPC protection analysis. G reaction (lane 1) and alkaline hydrolysis (lane 2) of a 3′-^{32}P end-labeled TAR are shown along the side of lanes 3−7 representing DEPC reaction of TAR in the presence of **3** at 0, 10, 50, 100, and 500 μM, respectively. (B) DMS protection analysis. DMS reactions of TAR in the presence of **3** at 0, 1, 5, 10, 50, 100, and 500 μM are shown in lanes 1−7, respectively. (C) V1 nuclease protection analysis. V1 cleavage reactions of a 5′-^{32}P end-labeled TAR in the presence of **3** at 0, 1, 10, 100, and 500 μM are shown in lanes 1−5, respectively. Lane 6 represents alkaline hydrolysis, and lane 7 represents G reaction of TAR.

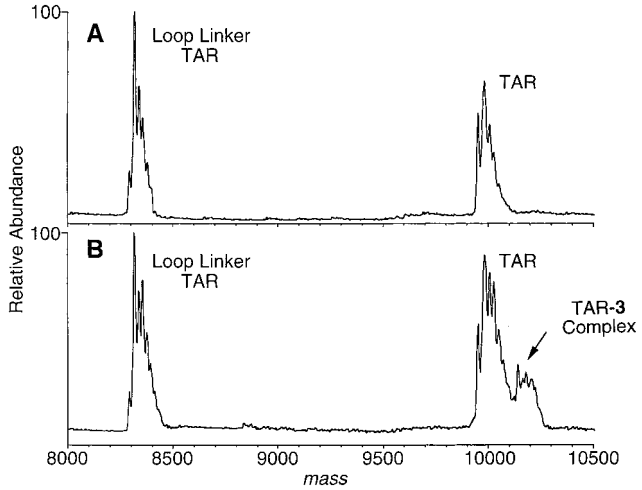

FIGURE 8: Deconvoluted negative ion ESI mass spectra of (A) wild type and loop linker TAR (1:1 molar ratio) and (B) wild type TAR, loop linker TAR, and **3** (1:1:2 molar ratio) (10 mM ammonium acetate at pH 6.9). Only the wild type TAR forms a noncovalent complex with **3**.

dent gene expression was also investigated. In this study, the expression of the *lacZ* gene is controlled by the cytomegalovirus (CMV) promoter, which does not contain the HIV-1 TAR element. In contrast to the results with LTR-activated *lacZ* expression, **3** shows no effect on the extent of gene expression driven by the CMV promoter. These results suggest that at least a portion of the cellular activity of **3** can be attributed to its inhibitory effect on Tat−TAR interaction.

Encouraged by its anti-Tat activity, we have further examined the ability of **3** to prevent the replication of HIV-1. OM-10.1 cells were used in this study because they are derived from HL-60 promyelocyte cells (*35*), which survive acute HIV-1 infection and contain an integrated copy of the HIV-1 genome. Significant HIV-1 gene expression in these cells occurs only upon induction by TNF-α. OM-10.1 has been used as a model cell line to represent transcriptional latency for HIV-1 since activation of these cells leads to expression of subgenomic RNAs encoding Tat and Rev proteins followed by a full length of genomic RNAs (*36*). The antiviral activity of **3** was determined by measuring the production of viral proteins p24. As shown in Figure 9B, **3** exhibits antiviral activity in the OM-10.1 cells with an EC_{50} value of 4 μM and a TC_{50} value of 54 μM. The antiviral activity of this compound in another HIV-1 chronically infected cell line, U1, has also been found. U1 cells are derived from U-937 promonocytic cells with an integrated

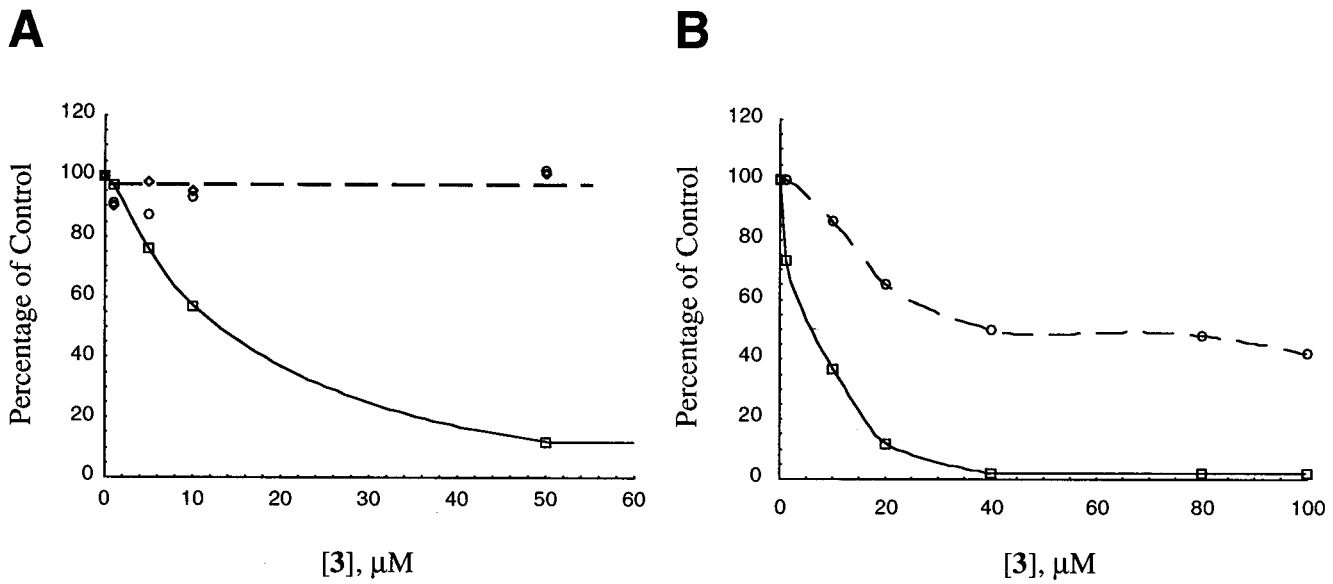

FIGURE 9: (A) Cellular Tat transactivation inhibited by **3**. A dose-dependent response of anti-Tat activity with **3** at increasing concentrations is shown (□). Below 50 μM, **3** shows no effects on either CMV-driven *lacZ* gene expression (◇) or the viability of the HeLa cells (○). (B) Anti-HIV-1 activity of **3**. Dose-dependent inhibition of HIV-1 replication in OM-10.1 cells by **3** is shown (□). Also shown is the effect of **3** on the cell viability (○).

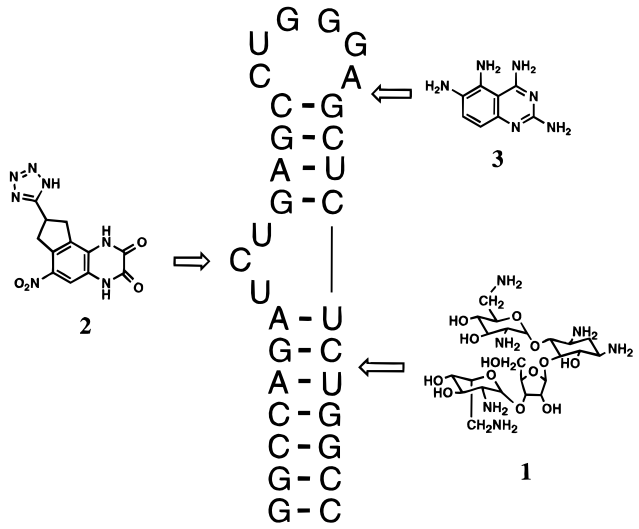

FIGURE 10: Primary binding sites of the three small molecule TAR ligands **1**−**3**.

HIV-1 genome (*37*). **3** inhibits HIV-1 replication in U1 cells with an EC_{50} of 16 μM. These results demonstrate that small molecule compounds identified and characterized as Tat−TAR inhibitors can inhibit the transcription of the HIV-1 gene in a relevant model system for viral replication.

Design Criteria for Improved Anti-HIV Drugs Based on TAR Recognition. We have identified three different small molecules that can inhibit HIV-1 Tat−TAR interaction by binding to the RNA component, TAR. Various methods have been applied to study the binding properties of these inhibitors. The results from all of these methods, not from each alone, reveal a unique mode of binding for each inhibitor. As shown in Figure 10, each of these small inhibitors recognizes a structurally different characteristic embedded in the RNA target. The primary binding sites of these molecules are the lower stem region for **1**, the bulge region for **2**, and the loop region for **3**. Structural studies using NMR or X-ray crystallography will be required to begin to understand the details of molecular interactions that are involved in these RNA−ligand interactions.

ESI-MS data suggest that **1** can bind to either free or Tat-bound TAR (*38*). This is quite interesting since a significant change in the structure of TAR induced by Tat has been shown (*39*, *40*). A reasonable explanation is that this conformational change is located at a site that does not affect the initial binding of **1**. Inspection of NMR structures of free and bound TAR (*33*) show that the double-helical stem regions, in particular the lower stem, are the least affected by the binding of Tat. Our footprinting data support this same binding characteristic in the case of **1**. Therefore, **1** provides an example for future drug design focusing on recognition at the double-helical region of TAR (*41*, *42*).

Our footprinting and dissociation kinetics results suggest that **2** binds to the bulge region of TAR. There is no apparent similarity between the structure of **2** and the arginine residue of Tat. It is likely that **2** recognizes different features in the bulge area, and that the conformation of the **2**−TAR complex can be different from that of Tat−TAR. In fact, biochemical (*43*) and NMR (*33*) studies have shown that the major groove around the bulge region of TAR is widened and unusually accessible to chemical reagents. This flexible, widened major groove can therefore provide a binding pocket not just for the protein but also for small molecules such as **2** whose binding will competitively displace Tat.

In addition to the lower stem and the bulge regions, another potential recognition site along TAR RNA is the highly flexible loop region. Although this region is not required for Tat binding (*14*−*16*), it is likely that small molecule loop binders can still interfere with Tat binding through an allosteric mechanism. The fact that **3** binds to the loop region and inhibits Tat−TAR binding provides encouragement for discovering ligands that bind to any loop-containing RNA molecules. Furthermore, the loop region of TAR has been shown to interact with cellular factors which are crucial for HIV-1 transcription (*12*). A loop binder like **3** or its derivatives might intercept interactions of TAR not only with

Tat but also with other cellular proteins.

Unlike the base-pairing rules used by nucleotide derivatives (for example, anti-sense DNA or RNA interact with template mRNA with typical Watson−Crick hydrogen bondings), there are no simple rules with which to predict the magnitude of small molecule interaction with RNA (*44*). This applies especially well to HIV-1 TAR, due to its dynamic behavior in solution. Evidence provided in this report and elsewhere (*33*) suggests that a conformational heterogeneity exists for TAR upon binding with various ligands. This could greatly limit the de novo approach in discovering new TAR ligands based on certain known TAR structures (free or Tat-bound TAR) but not the random screening approach. The results presented here demonstrate the feasibility of the latter approach. As in any drug screening programs, leads **1**−**3** may not prove to be the ultimate clinical candidates for treating HIV-1 infection; however, they do provide reasonable templates for further developing TAR ligands with improved efficiency and selectivity. In one example, we have identified a RNA ligand capable of inhibiting the functions of its RNA target in a purified protein−RNA system as well as in HIV-1-infected cellular environments. Although the detailed cellular mechanism of this RNA ligand is not known, a strong correlation does exist among its activity in Tat−TAR inhibition, TAR-dependent cellular Tat transactivation, and anti-HIV-1 replication in a transcription-based latency model. Further investigation of these RNA ligands and their derivatives is required for better understanding of small molecule−RNA interactions and their efficacies in HIV-1 therapy.

ACKNOWLEDGMENT

We thank our colleagues Drs. D. Mack, D. Moreland, S. Brown, J. Domagala, and S. Gracheck for helpful discussions. We benefited significantly from Drs. D. Crothers, G. Glick, C. Chow, J. SantaLucia, and P. Toogood through their consultations at the early stage of this project. We also thank Drs. J. Bristol and L. Post for their leadership and support.

REFERENCES

1. Matthews, J. C. (1993) *Fundamentals of Receptor, Enzyme, and Transport Kinetics*, pp 1−22, CRC Press Inc., Boca Raton, FL.
2. Bass, B. L., and Cech, T. R. (1984) *Nature 308*, 820−826.
3. Gottesfeld, J. M., Neely, L., Trauger, J. W., Baird, E. E., and Dervan, P. B. (1997) *Nature 387*, 202−205.
4. Westhof, E., Masquida, B., and Jaeger, L. (1996) *Folding Des. 1*, R78−R88.
5. Dingwall, C., Ernberg, I., Gait, M. J., Green, S. M., Heaphy, S., Karn, J., Lowe, A. D., Singh, M., Skinner, M. A., and Valerio, R. (1990) *EMBO J. 9*, 4145−4153.
6. Cech, T. R. (1990) *Annu. Rev. Biochem. 59*, 543−568.
7. Michel, F., and Westhof, E. (1990) *J. Mol. Biol. 216*, 585−610.
8. Cullen, B. R. (1994) *Infect. Agents Dis. 3*, 68−76.
9. Harrich, D., Mavankal, G., Mette-Snider, A., and Gaynor, R. B. (1995) *J. Virol. 69*, 4906−4913.
10. Muesing, M. A., Smith, D. H., and Capon, D. J. (1987) *Cell 48*, 691−701.
11. Feng, S., and Holland, E. C. (1988) *Nature 334*, 165−167.
12. Hauber, J., Malim, M. I. I., and Cullen, B. R. (1989) *J. Virol. 63*, 1181−1187.
13. Calnan, B. J., Tidor, B., Biancalana, S., Hudson, D., and Frankel, A. D. (1991) *Science 252*, 1167−1171.
14. Sheline, C. T., Milocco, L. H., and Jones, K. A. (1989) *Genes Dev. 5*, 2508−2520.
15. Marciniak, R. A., Garcia-Blanco, M. A., and Sharp, P. A. (1990) *Proc. Natl. Acad. Sci. U.S.A. 87*, 3624−3628.
16. Hamy, F., Felder, E. R., Heizmann, G., Lazdins, J., Aboul-Ela, F., Varani, G., Karn, J., and Klimkait, T. (1997) *Proc. Natl. Acad. Sci. U.S.A. 94*, 3548−3553.
17. Gait, M. J., and Karn, J. (1995) *Trends Biotechnol. 13*, 430−438.
18. Li, C. J., Dezube, B. J., Biswas, D. K., Ahlers, C. M., and Pardee, A. B. (1994) *Trends Microbiol. 2*, 164−169.
19. Mei, H.-Y., Mack, D. P., Galan, A., Halim, N., Heldsinger, A., Loo, J., Moreland, D., Sannes, K., Sharmeen, L., Truong, H. N., and Czarnik, A. W. (1997) *Bioorg. Med. Chem. 5*, 1173−1184.
20. Moazed, D., and Noller, H. F. (1987) *Nature 327*, 389−394.
21. Schroeder, R., and Von Ahsen, U. (1996) *Nucleic Acids Mol. Biol. 10*, 53−74.
22. Shu, Y.-Z., Ye, Q., Li, H., Kadow, K. F., Hussain, R. A., Huang, S., Gustavson, D. R., Lowe, S. E., Chang, L.-P., Pirnik, D. M., and Kodukula, K. (1997) *Bioorg. Med. Chem. Lett. 7*, 2295−2298.
23. Lim, A. C., and Barton, J. K. (1997) *Bioorg. Med. Chem. 5*, 1131−1136.
24. Zapp, M. L., Young, D. W., Kumar, A., Singh, R., Boykin, D. W., Wilson, W. D., and Green, M. R. (1997) *Bioorg. Med. Chem. 5*, 1149−1155.
25. Li, K., Fernandez-Saiz, M., Rigl, C. T., Kumar, A., Ragunathan, K. G., McConnaughie, A. W., Boykin, D. W., Schneider, H.-J., and Wilson, W. D. (1997) *Bioorg. Med. Chem. 5*, 1157−1172.
26. Hamy, F., et al. (1998) *Biochemistry 37*, 5086−5095.
27. Siuzdak, G. (1994) *Proc. Natl. Acad. Sci. U.S.A. 91*, 12290−12297.
28. Loo, J. A. (1995) *Bioconjugate Chem. 6*, 644−665.
29. Mei, H.-Y., Galan, A. A., Halim, N. S., Mack, D. P., Moreland, D. W., Sanders, K. B., Truong, H. N., and Czarnik, A. W. (1995) *Bioorg. Med. Chem. Lett. 5*, 2755−2760.
30. Sannes-Lowery, K. A., Hu, P., Mack, D. P., Mei, H.-Y., and Loo, J. A. (1997) *Anal. Chem. 69*, 5130−5135.
31. Wang, S., Huber, P. W., Cui, M., Czarnik, A. W., and Mei, H.-Y. (1998) *Biochemistry 37*, 5549−5557.
32. Stern, S., Moazed, D., and Noller, H. F. (1988) *Methods Enzymol. 164*, 481−489.
33. Aboul-ela, F., Karn, J., and Varani, G. (1996) *Nucleic Acids Res. 24*, 3974−3981.
34. Loo, J., Sannes, K., Hu, P., Mei, H.-Y., and Mack, D. (1997) in *NATO ASI Series on New Methods for the Study of Molecular Aggregates* (Standing, K. G., and Ens, W., Eds.) Kluwer Academic Publishers, Dordrecht, The Netherlands (in press).
35. Butera, S. T., Perez, V. L., Wu, B. Y., Nabel, G. J., and Folks, T. M. (1991) *J. Virol. 65*, 4645−4653.
36. Adams, M., Sharmeen, L., Kimpton, J., Romeo, J. M., Garcia, J. V., Peterlin, B. M., Groudine, M., and Emerman, M. (1994) *Proc. Natl. Acad. Sci. U.S.A. 91*, 3862−3866.
37. Folks, T. M., Justement, J., Kinter, A., Dinarello, C. A., and Fauci, A. S. (1987) *Science 238*, 800−802.
38. Sannes-Lowery, K. A., Mei, H.-Y., Mack, D., and Loo, J. A. (1997) *Proceedings of the 45th ASMS Conference on Mass Spectrometry and Allied Topics*, p 1390, Palm Springs, CA.
39. Puglisi, J. D., Tan, R., Canlan, B. J., Frankel, A. D., and Williamson, J. R. (1992) *Science 257*, 76−80.
40. Aboul-ela, F., Karn, J., and Varani, G. (1995) *J. Mol. Biol. 253*, 313−332.
41. McConnaughie, A. W., Spychala, J., Zhao, M., Boykin, D., and Wilson,W. D. (1994) *J. Med. Chem. 37*, 1063−1069.
42. Fourmy, D., Recht, M. I., Blanchard, S. C., and Puglisi, J. D. (1996) *Science 274*, 1367−1371.
43. Weeks, K. M., and Crothers, D. M. (1991) *Cell 66*, 577−588.
44. Chow, C. S., and Bogdan, F. M. (1997) *Chem. Rev. 97*, 1489−1513.

BI981308U